J. Fluid Mech. (1986), *vol.* 173, *pp.* 207–223
Printed in Great Britain

A series-expansion study of the Navier–Stokes equations with applications to three-dimensional separation patterns

By A. E. PERRY AND M. S. CHONG
Mechanical Engineering Department, University of Melbourne, Parkville, Victoria 3052, Australia

(Received 25 March 1986)

An algorithm has been developed which enables local Taylor-series-expansion solutions of the Navier–Stokes and continuity equations to be generated to arbitrary order. Much of the necessary algebra for generating these solutions can be done on a computer. Various properties of the algorithm are investigated and checked by making comparisons with known solutions of the equations of motion. A method of synthesizing nonlinear viscous-flow patterns with certain required properties is developed and applied to the construction of a number of two- and three-dimensional flow-separation patterns. These patterns are asymptotically exact solutions of the equations of motion close to the origin of the expansion. The region where the truncated series solution satisfies the full equations of motion to within a specified accuracy can be found.

1. Introduction

This work grew out of a desire to study the topology and geometry of complex three-dimensional steady and unsteady flow patterns and eddying motions. Critical-point theory has, in the past, been used for describing and classifying flow patterns. A critical point in a flow field is a point where the streamline slope is indeterminate, i.e. $(u_i/u_j) = 0/0$ where $i \neq j$ and u_i is the velocity. By Taylor-series expanding the velocity field u_i about the critical point in terms of the space coordinate x_j and substituting the expansion into the Navier–Stokes and continuity equations, certain relationships between the coefficients of the expansion can be found. All possible patterns close to a critical point can be derived and classified. Sectional streamline patterns form saddles, nodes or foci. Oswatitsch (1958) was the first to carry out a systematic analysis of critical points located at a no-slip boundary and derived the various three-dimensional separating and reattaching flows close to such points. Lighthill (1963) discussed further the solutions of Oswatitsch, and Perry & Fairlie (1974) applied phase-plane techniques to the description of critical points. Critical points that occur away from no-slip boundaries (the so-called free-slip critical points) require different formulations and have been studied by Perry and Fairlie (1974) and recently, in greater detail, by Perry (1984*a*).

Critical points are the salient features of a flow pattern. If their position and type is known, the rest of the pattern can be deduced qualitatively, since there are a limited number of ways that the streamlines can be joined between the points. The basic topology and qualitative transport properties of the pattern can be understood by using the critical-point concept.

A series expansion up to second order about a critical point (e.g. the Oswatitsch solution) is limited to describing the flow in the immediate vicinity of the critical point. Dallmann (1983) has recently shown that if the series expansion can be extended to higher orders, a flow field consisting of a cluster of critical points can be described in one formulation. One major difficulty is the large amount of labour required in deriving the formulations.

Therefore the aim is to develop an algorithm that will enable local solutions of the Navier–Stokes and continuity equations to be generated to arbitrary order and, as far as possible, the computer is to be used to carry out the necessary algebra. A further aim is to apply the algorithm to the study of three-dimensional separation patterns of the type recently observed and classified by Bippes & Turk (1983) and Hornung & Perry (1984) and discussed by Dallmann (1983).

The series expansion can be applied to any point in the flow field (i.e. not necessarily at a critical point) and the algorithm or some modified version of it might, in the future, form the basis of a computational scheme. The Taylor-series expansion is probably not the optimum form of series to use in computational methods. However, in this paper the algorithm is being used as a tool for investigating the properties of the Navier–Stokes and continuity equations and the topological features of flow patterns.

The work is based in part on that by Perry (1984*b*). However, many of the initial ideas expressed by Perry, particularly the problems with convergence and boundary conditions, have been revised in this paper. A preliminary report on this work was given by Perry, Chong & Hornung (1985).

2. Theory

The Navier–Stokes equations for incompressible, constant-density flow can be expressed as a single tensor equation thus:

$$\frac{\partial u_i}{\partial t}+u_q\frac{\partial u_i}{\partial x_q}=-\frac{\partial P}{\partial x_i}+\nu\frac{\partial^2 u_i}{\partial x_q\,\partial x_q}, \tag{1}$$

where $P=p/\rho$ is the kinematic pressure, p is the pressure, ρ is the fluid density, ν is the kinematic viscosity, u_i is the velocity tensor and x_i is the space coordinate tensor (Cartesian coordinates). The continuity equation is

$$\frac{\partial u_i}{\partial x_i}=0. \tag{2}$$

Let us expand the velocity field thus:

$$u_i=A_i+A_{ij}x_j+A_{ijk}x_j x_k+A_{ijkl}x_j x_k x_l+A_{ijklm}x_j x_k x_l x_m+\ldots. \tag{3}$$

Equation (3) will be substituted into (1) and (2). There are certain properties of (3) that should be exploited to simplify the analysis. All coefficients in (3) are symmetric in all indices but the first, e.g. $A_{ijkl}=A_{ilkj}=A_{ikjl}$, etc. Equation (3) could be written as

$$u_i=\sum_{n=0}^{N} RA_{i(111\ldots,\,222\ldots,\,333\ldots)}\,x_1^a\,x_2^b\,x_3^c, \tag{4}$$

where $a+b+c=n$ in every possible combination and permutation. a, b and c are positive whole numbers or zero. R = number of possible permutations of the indices in $(111\ldots,222\ldots,333\ldots)$ where 1 is repeated 'a' times, 2 is repeated 'b' times and 3 is repeated 'c' times. In fact $R=(a+b+c)!/a!\,b!\,c!$

It can be shown that the number of unknown coefficients for an Nth-order series expansion is

$$N_c = 3 \sum_{K=0}^{N} \sum_{J=0}^{K+1} J. \tag{5}$$

The generation of relationships for the unknown coefficients as given by the continuity and Navier–Stokes equations is rather lengthy, and full technical details are given in Perry (1984*b*) and Perry & Chong (1986). A brief outline is as follows.

Substituting (3) into (2) and equating coefficients of like powers for various powers n generates no equations for $n = 0$, one equation for $n = 1$, three non-redundant equations for $n = 2$, six non-redundant equations for $n = 3$ and so on to higher powers. For example, for $n = 4$, the continuity equation is

$$A_{11\alpha\beta\gamma} + A_{22\alpha\beta\gamma} + A_{33\alpha\beta\gamma} = 0, \tag{6}$$

and this gives 10 non-redundant equations. It can be shown that the number E_c of non-redundant continuity equations generated for an Nth-order expansion is

$$E_c = \sum_{n=0}^{N} \sum_{J=0}^{n} J. \tag{7}$$

If the series expansion (3) is substituted into (1) and the terms of the same order are grouped, P_r, the rth derivative of pressure at the origin of the expansion, can be found. For example, P_3 is given by

$$\frac{\partial^3 P}{\partial x_\beta \partial x_\alpha \partial x_i}(O) = -2\dot{A}_{i\alpha\beta} - 6[A_q A_{i\alpha\beta q} + 2(A_{iq} A_{q\alpha\beta} + A_{q\alpha} A_{i\beta q} + A_{q\beta} A_{i\alpha q})] + 24\nu A_{i\alpha\beta qq} \tag{8}$$

and this is a third-order tensor. The symbol (O) means 'at the origin'. In general, the various P_rs are given by

$$P_r = -(r-1)!\,\dot{\boldsymbol{r}} - [\sum_{C(J+K=r+2)} (J-1)!\,(K-1)!\,\boldsymbol{J}\cdot\boldsymbol{K}] + \nu(r+1)!\,\boldsymbol{r}. \tag{9}$$

The three terms on the right-hand side of (9) come from the time derivative, convective and viscous terms respectively in the Navier–Stokes equations (1).

Consider first the convective term shown in square brackets. The symbol $\Sigma_{C(J+K=r+2)}$ means to sum up over all possible combinations of J and K excluding zero values of J and K. The symbols $\boldsymbol{J}$ and $\boldsymbol{K}$ denote Jth-order and Kth-order tensors. The combination $\boldsymbol{J}\cdot\boldsymbol{K}$ denotes the sum of products of Jth- and Kth-order tensors and the number of free indices in each product is r. In each combination $\boldsymbol{J}\cdot\boldsymbol{K}$, q, the index defined in (1), always leads the indices of one tensor and i always leads the indices of the other. There are always 2 qs in each combination and they never occur together in one tensor. Whenever there is an i in a tensor, it must always be accompanied by a q in the same tensor. The free indices i, α, β, δ, etc. must be cycled so that they appear in all possible combinations in each tensor, and this must be done while observing the above rules.

The rule for formulating the time derivative $\dot{\boldsymbol{r}}$ is that this is an rth-order tensor $\dot{A}_{i\ldots\lambda\delta\beta\alpha}$. No qs are involved. The viscous-term tensor $\boldsymbol{r}$ is an rth-order tensor with a leading index i and a repeated index q, i.e. $\boldsymbol{r} = A_{i\ldots\lambda\delta\beta\alpha qq}$ and there are r free indices. All the above is best understood by considering (8) as an example. With $r = 3$, (9) becomes

$$P_3 = -2!\,\dot{\mathbf{3}} - 0!\,3!\,\mathbf{1}\cdot\mathbf{4} + 1!\,2!\,\mathbf{2}\cdot\mathbf{3} + 4!\,\nu\,\mathbf{3}.$$

Now $\dot{\mathbf{3}}$ means $\dot{A}_{i\alpha\beta}$ and **3** in the viscous term means $A_{i\alpha\beta qq}$. In the convective terms $0!3!\mathbf{1\cdot4}$ means $6A_qA_{i\alpha\beta q}$ and the symbol $1!2!\mathbf{2\cdot3}$ means $2(A_{iq}A_{q\alpha\beta}+A_{q\alpha}A_{i\beta q}+A_{q\beta}A_{i\alpha q})$. All of this leads to (8). In general, to obtain the rth derivative of pressure the order N of the series expansion must be such that $N \geqslant r+1$ so that appropriate viscous terms are generated in (9).

The various orders of pressure derivatives can now be generated and appropriate cross-derivatives can be equated within each order. These then generate equations that give relationships between the various coefficients. The equating of cross-derivatives commences at the second derivatives and proceeds to the higher derivatives. In this procedure, many equations that are generated are redundant. However, it can be shown that the number of non-redundant equations generated by an Nth-order series expansion is

$$E_{\mathrm{NS}} = \sum_{n=3}^{N} \sum_{J=2}^{n-1} (2J-1), \tag{10}$$

where E_{NS} is the total number of Navier–Stokes equations generated. In fact, since pressure has been eliminated, we are effectively constructing vorticity transport equations to various orders, and these turn out to be first-order ordinary differential equations for the series-expansion coefficients. Hence, with the aid of the algorithm developed, it is possible to generate all the Navier–Stokes and continuity relationships between the coefficients to any order. The authors have developed a computer program that generates the equations because of the enormous amount of algebra required.

By a similar analysis to that used for the Navier–Stokes equation, it is found that

$$E_{\mathrm{E}} = \sum_{n=2}^{N} \sum_{J=2}^{n} (2J-1), \tag{11}$$

where E_{E} is the number of equations generated by the Euler equation.

The corresponding set of equations for two-dimensional flow is as follows:

$$\left.\begin{aligned} N_{\mathrm{c}} &= 2\sum_{J=1}^{N+1} J, \\ E_{\mathrm{C}} &= \sum_{J=0}^{N} J, \\ E_{\mathrm{NS}} &= \sum_{J=2}^{N-1} (J-1), \\ E_{\mathrm{E}} &= \sum_{J=2}^{N} (J-1). \end{aligned}\right\} \tag{12}$$

Table 1 summarizes the number of unknowns and equations generated. This gives an idea of the complexity of the problem and shows the need for computer-generated algebra. It also shows that three-dimensional flow is an order of magnitude more complex than two-dimensional flow.

It can be seen from the tabulation that the number of unknowns always exceeds the number of equations generated. Hence, in order to obtain a solution, additional equations must be supplied from boundary conditions. If the flow is unsteady, these boundary conditions must be known functions of time which become forcing functions for the ordinary differential equations. Also, all coefficients must be known at some initial time. In steady flow (which will be our main concern here) the problem

Two-dimensional					Three-dimensional				
N	N_c	E_c	E_{NS}	E_E	N	N_c	E_c	E_{NS}	E_E
0	2	0	0	0	0	3	0	0	0
1	6	1	0	0	1	12	1	0	0
2	12	3	0	1	2	30	4	0	3
3	20	6	1	3	3	60	10	3	11
4	30	10	3	6	4	105	20	11	26
5	42	15	6	10	5	168	35	26	50
.	.	.	.	.	.	.	.	.	.
.	.	.	.	.	.	.	.	.	.
15	272	120	91	105	15	2448	680	1001	1225

TABLE 1. Number of unknowns and equations

is to solve a set of simultaneous algebraic equations. The continuity relationships are simple linear algebraic equations and the Navier–Stokes relationships consist of linear (viscous) terms and quadratic (convective) terms.

Once the velocity field has been determined, the pressure field P can be found from (9), since

$$P = P_O + P_1 x_i + P_2 \frac{x_i x_\alpha}{2!} + P_3 \frac{x_i x_\alpha x_\beta}{3!} + \ldots . \tag{13}$$

This must truncate at the P_{N-1} term. P_O is the kinematic pressure at the origin.

The equations, rules and procedures outlined in this section will be referred to as the 'algorithm'.

3. Testing the algorithm

Perry (1984*b*) has tested the above algorithm by hand up to fourth order using a number of simple three-dimensional test cases which have known solutions, e.g. the solutions given by Perry (1984*a*) and Hornung (1983). Following on from this work, the authors have developed computer programs which in principle can generate the necessary equations up to arbitrary order. Results of a preliminary investigation are presented here where a known steady two-dimensional solution is used for testing the algorithm up to ninth order. A simple potential flow has been chosen and is shown in figure 1. It should be kept in mind that potential flow is an exact solution of the Navier–Stokes and continuity equations, and the algorithm will be applied to this flow without any assumption of irrotationality. The flow consists of a pair of point vortices convecting through stationary fluid at a velocity U_∞. If the observer moves with the vortex pair, a steady pattern is produced. In figure 1, various parameters of the flow are defined. The exact solution is series expanded about a point in the flow, and this is used for generating boundary conditions. These boundary conditions are specified as one-dimensional series expansions, i.e. along lines, for two-dimensional flows (and as two-dimensional series expansions, i.e. in planes, for three-dimensional flows). The boundary conditions are then used in the algorithm for determining the solution. This is compared with the original exact solution.

It has been found that in steady-flow patterns, certain boundary-condition specifications lead to a very simple solution procedure. Because of the sequence in which certain coefficients are determined, the procedure leads to sets of Navier–Stokes relationships which are linear in the remaining unknown coefficients (all quadratic

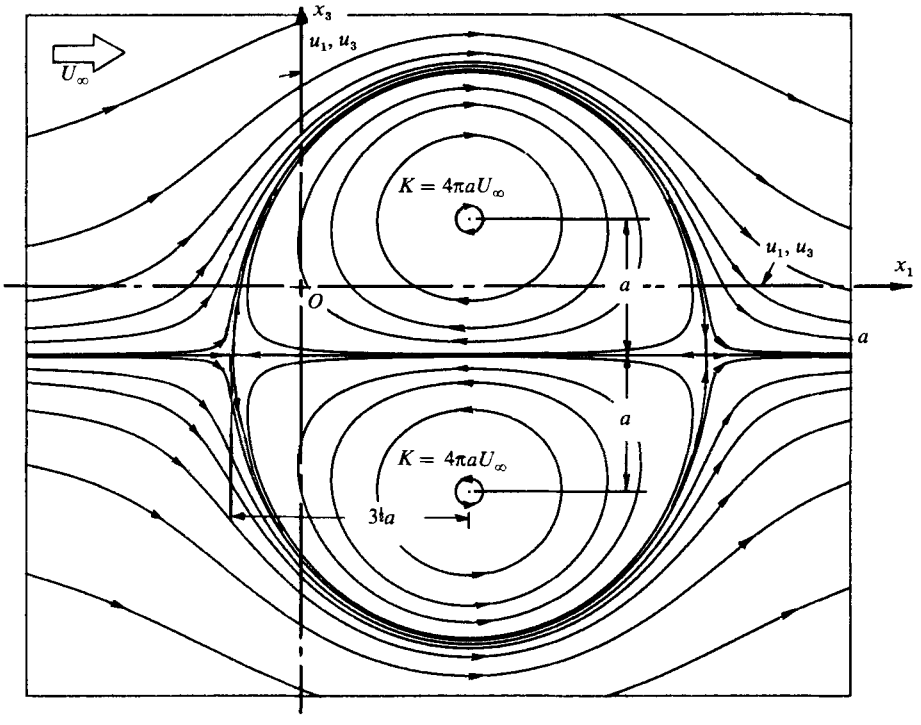

FIGURE 1. Two-dimensional potential-flow pattern used as a test case. K = circulation.

terms contain at least one known coefficient). All equations are then effectively linear in terms of the coefficients and can be solved by substitution. In other types of boundary-condition specifications, the Navier–Stokes-generated relationships remain nonlinear with terms involving products of unknown coefficients. In some cases, the difficulty with the nonlinearity can be overcome by solving the problem as a time-dependent one where we march in time and the various coefficients are updated by simple substitution without any iterative procedure at the end of each timestep.

The specification of boundary conditions as a series introduces problems of redundancy. Certain coefficients determined from boundary conditions must also satisfy the equations of motion, otherwise a contradiction occurs. In all computations carried out, coefficients determined from the equations of motion take priority if the same coefficients can also be determined from boundary conditions. These redundant boundary-condition equations are ignored. Other methods of specifying boundary conditions are being explored. For instance, it is possible to specify boundary conditions on four sides of a box, and the polynomials used for these boundary conditions are generated from a series expansion about the origin which is inside the box. These polynomials have 'boundary coefficients' which are related to the velocity-field coefficients. If we specify only some of the lower-order boundary coefficients on all four sides of the box, it is possible to generate sufficient equations to obtain closure, but the Navier–Stokes relationships become nonlinear in the remaining unknown coefficients. This is somewhat analogous to specifying boundary conditions at grid points around the perimeter of a finite domain, as is usually done in conventional numerical methods. The authors have not yet found a way of overcoming this difficulty of nonlinearity even when solving the problem as a

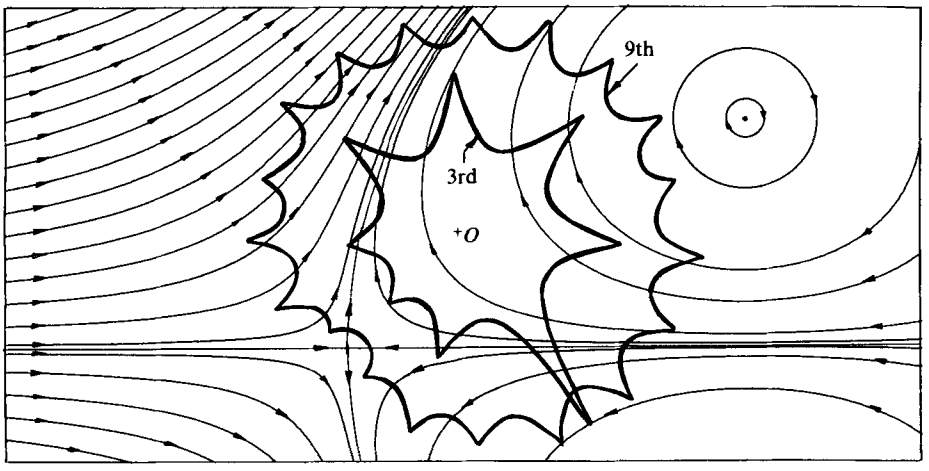

FIGURE 2. Comparison 1 for expansion about point O.

time-dependent one. It would appear that iterative methods would need to be employed. This is still being pursued. For the purpose of this preliminary investigation the boundary conditions shown in figure 1 are used where the 'boundaries' pass through the origin of the series expansion. This leads to what the authors refer to as a 'canonical' set of boundary conditions, since each of the boundary-condition equations generated has only one unknown. This greatly simplifies the solution procedure and leads effectively to a linear set of equations as mentioned earlier.

Consider a solution about O in figure 1. The boundary conditions are specified by specifying u_1 and u_3 along two mutually perpendicular lines passing through O. For an Nth-order series expansion, these boundary conditions are specified as an Nth-order series expansion about O. The region where the full Navier–Stokes and continuity equations agree with the generated truncated set of equations (the region of accuracy) will be a finite zone surrounding the point O.

Various methods have been developed for determining the boundary of this region of accuracy. Figure 2 shows such boundaries for a 3rd- and 9th-order series expansion about an arbitrarily chosen point O. The origin O does not necessarily need to be located at a critical point. Here a comparison is made with the velocity magnitude given by a series expansion of the exact known solution and the full exact known solution. This will be referred to as comparison 1. The boundaries represent a 1% departure in velocity magnitude. The boundaries are insensitive to the fractional error chosen since, once a departure occurs, it grows very rapidly with radial distance from O. It can be seen that the region of accuracy grows as the order of the expansion increases.

In figure 3, the boundary conditions have been substituted into the algorithm and comparisons are made between two pressure distributions. This will be referred to as comparison 2. The first pressure field is given by the truncated series expansion (13). The second pressure field is obtained by substituting the velocity-field solution into the full Navier–Stokes equations. The boundary represents $2\delta P/U_\infty^2 \leqslant 5\%$, where δP is the departure in pressure given by the two methods. This method of comparison has the advantage that one does not need to know the exact solution *a priori*. This method is applied later to the separation-bubble computations. It should be noted from figure 3 that the boundary depends on Reynolds number Re. For $Re = aU_\infty/\nu = 100$, the region of accuracy is close to that given in figure 2. However,

FIGURE 3. Comparison 2 for expansion about point O.

as the Reynolds number is increased, the region of accuracy shrinks. The region of accuracy of the computed solution is governed by two effects. One effect is caused by the fact that we are using a truncated series expansion; the other is caused by rounding errors. For comparison 2 in figure 3, at a Reynolds number of 100, truncation errors are the dominant source of departure, but as the Reynolds number increases rounding errors become equally important. This was confirmed by computing and specifying the boundary conditions in double precision. The region of accuracy for the higher Reynolds numbers increased appreciably. The source of rounding errors is in the convective terms for vorticity. These theoretically should sum to zero for irrotational flow but have a small error ϵ. The terms involving the vorticity diffusion are equal to ϵ/ν. Theoretically these should sum to zero for irrotational flow, but as $\nu \to 0$ this quantity becomes unbounded. The authors suspected that perhaps there were programming errors in the computation of the convective terms. This was found not to be so by using the algorithm for solving the Euler equation about O. The numerical rounding errors become negligible. Hence the Navier–Stokes equations are more prone to rounding errors than the Euler equations. How the rounding errors affect the region of accuracy is still being investigated.

A more convenient comparison has been developed and is closely related to comparison 2. From the truncated set of equations, the truncated value of |grad P|, i.e. $|\nabla P|_{\mathrm{T}}$ can be computed from (13). The truncated solution to the velocity field is then substituted into the full Navier–Stokes equations and the |grad P| given by this, i.e. $|\nabla P|_{\mathrm{F}}$ can be compared with $|\nabla P|_{\mathrm{T}}$. A suitable criterion for the region of accuracy can be formulated as follows:

$$\frac{|\nabla P|_{\mathrm{F}} - |\nabla P|_{\mathrm{T}}}{|\nabla P|_{\mathrm{F}}} \leqslant 10\,\%. \tag{14}$$

This will be called comparison 3, and cursory checks gave similar results to the other comparisons.

4. Flow pattern synthesis in two dimensions

As was stated in the Introduction, the initial aim of this work was to explore three-dimensional steady and unsteady flow-pattern topology. Producing separation patterns of various desired shapes and sizes by specifying boundary conditions is a very difficult and time-consuming procedure. Using the algorithm in conjunction with critical-point theory, the authors have discovered how to generate separation patterns with great control over their scale and topological properties. These patterns are solutions of the Navier–Stokes and continuity equations to a given order, and their region of accuracy is very simple to determine using the methods outlined in §3. Not only are these solutions useful as research tools in flow-pattern topology, but they might be useful for generating boundary conditions for the purpose of testing various computational methods. The synthesis of a simple two-dimensional steady fifth-order separation bubble will first be considered.

Imagine we have a no-slip boundary along which we will specify the boundary vorticity $\eta = (u_1/x_3)_{x_3 \to 0}$ to vary according to the equation

$$\eta = K(x_1^2 - x_s^2) \tag{15}$$

This is illustrated in figure 4. This gives two critical points on the wall at points 1 and 2 which are saddles. In fact, the solutions to second order are known close to the critical points. A local series expansion about point 1 in figure 4 in terms of $\hat{x}_1$ and x_3 gives

$$\begin{bmatrix} u_1/x_3 \\ u_2/x_3 \end{bmatrix} = \begin{bmatrix} 2Kx_s & B \\ 0 & -Kx_s \end{bmatrix} \begin{bmatrix} \hat{x}_1 \\ x_3 \end{bmatrix}, \tag{16}$$

where the coordinate origin is now at the critical point. This is the well-known Oswatitsch (1958) solution and has been discussed by Perry & Fairlie (1974), Hornung & Perry (1984) and by Perry (1984*a*) including the extension to three dimensions. The angle at which the separating or reattaching streamline leaves the surface is given by

$$\tan\theta = \frac{3Kx_s}{B}, \tag{17}$$

where B is the local streamwise pressure derivative parameter $\frac{1}{2}\partial P/\partial x_1$ and $2Kx_s$ is the streamwise gradient of wall vorticity, i.e. η_{x_1}. A similar expansion is carried out about point 2.

By specifying η, θ_1 and θ_2 we generate equations which replace the conventional boundary-condition equations. Used in conjunction with the algorithm to fifth order, it turns out that to obtain closure we can choose the position of a third critical point, i.e. point 3 in figure 4. Once this point is specified, the pattern is fixed. Figure 5 shows some typical patterns. In figure 5(*a*) the critical point 3 was chosen too far from the surface to give a closed bubble. In figure 5(*b*), point 3 has been shifted closer to the surface and a closed bubble is produced. Note that an extra saddle appears in the pattern. In figure 5(*c*) the Reynolds number $Re = Kx_s^2/\nu$ has been reduced from 50 to 10 and the extra saddle has moved out of 'view'. The region of accuracy of these solutions has been computed using comparison 2 in §3. A characteristic pressure variation through the pattern is given by $\Delta P = 4\nu B x_s$ and from (16) an appropriate accuracy criterion to use is that

$$\frac{\delta P}{\Delta P} = \frac{\delta P \tan\theta_1}{12\nu K x_s} \leqslant 5\,\%. \tag{18}$$

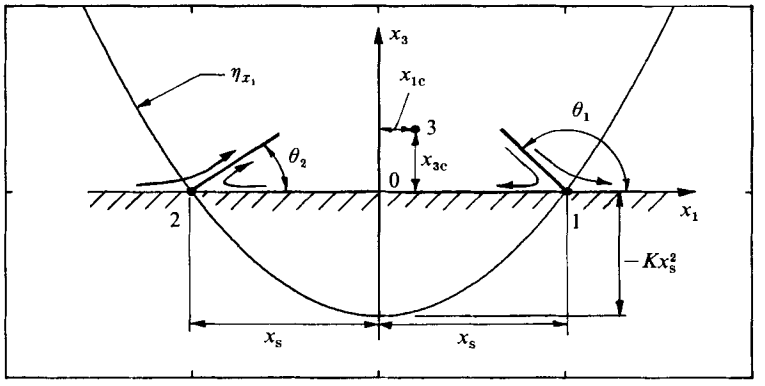

FIGURE 4. Parameters used in the synthesis of a two-dimensional bubble.

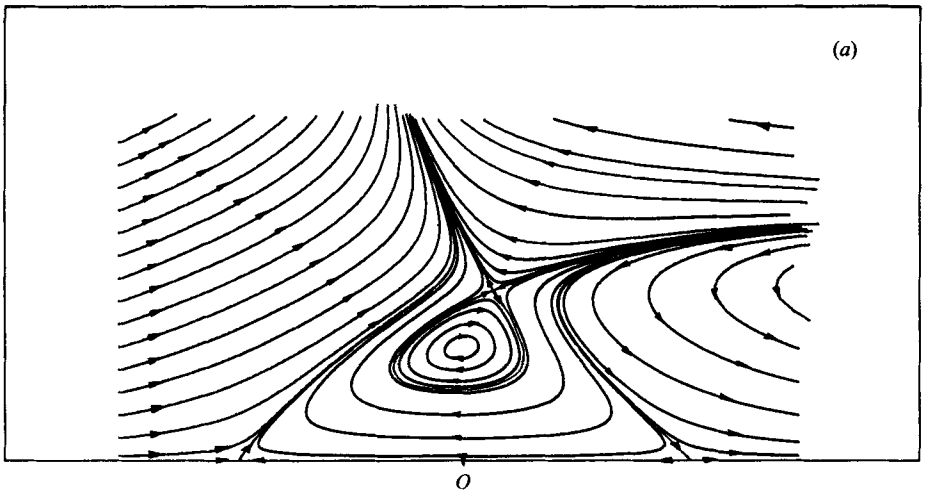

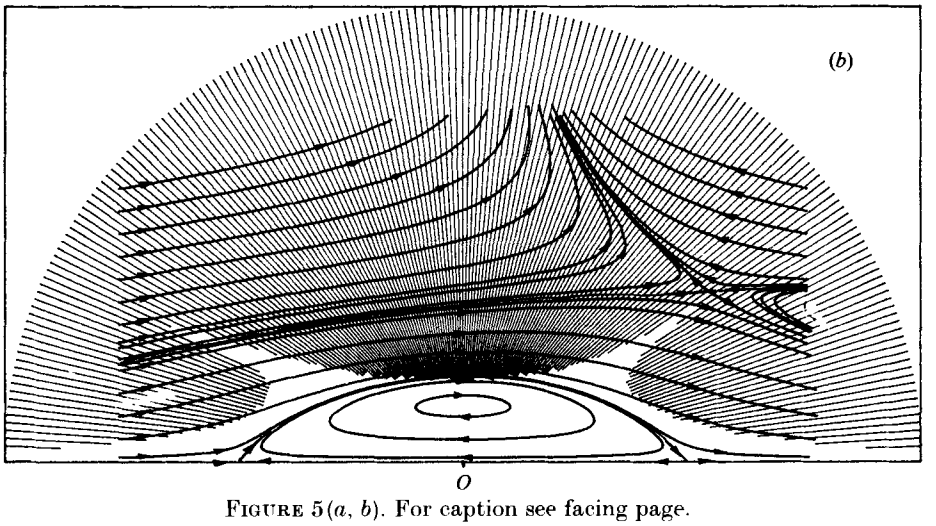

FIGURE 5(*a*, *b*). For caption see facing page.

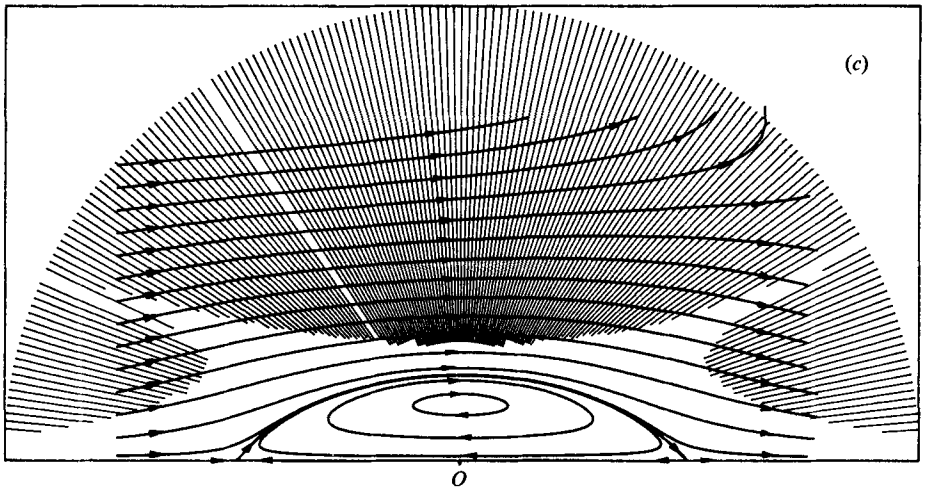

FIGURE 5. Fifth-order two-dimensional separation bubble. $K = 0.5$, $\theta_1 = 135$, $\theta_2 = 45$, $x_s = 1$. (*a*) Location of centre $x_{1c} = 0$, $x_{3c} = 0.5$, $Re = 50$. (*b*) Location of centre $x_{1c} = 0$, $x_{3c} = 0.25$, $Re = 50$. (*c*) As in (*b*) but with $Re = 10$. Region of accuracy shown unshaded in (*b*) and (*c*).

The region of accuracy using this criterion is shown in figure 5(*b*, *c*). As an additional check on the algorithm, these solutions were used to generate boundary conditions for u_1 and u_2 along the x_1 and x_3 axes. These were then used with the algorithm, and the resulting solution agreed with the synthesized solution to great accuracy over the entire flow field.

5. Synthesis of three-dimensional separation patterns

Using a similar technique as for the two-dimensional synthesis, a more general procedure has been developed for the synthesis of three-dimensional-flow separation. The surface vorticity must first be specified. By shifting the origin of the series expansion to various critical points located on the surface and by specifying the properties of these critical points, sufficient equations relating the various coefficients can be generated which allow the surface flow patterns to be synthesized. The flow pattern above the surface that would generate a particular type of surface flow pattern is not unique, and a variety of separation flow patterns could be generated. Further conditions need to be specified. These conditions are usually the angles of separation and reattachment and various locations and properties of critical points above the surface. In general, the higher the order of the series expansion, the more conditions need to be specified for closure (remembering, as discussed in §2, that all the Navier–Stokes and continuity relationships generated must be used).

Examples of various separation bubbles are shown in figures 6, 7 and 8. A full description of the properties and numerical values of the various parameters for these patterns are given in Perry & Chong (1986). The surface flow patterns (limiting streamlines in the (x_1, x_2)-plane) shown in the figures are those which have been classified as U-separation, owl-face of the first kind, and owl-face of the second kind by Hornung & Perry (1984) and Perry & Hornung (1984) from surface dye-trace observations of flow behind missile-shaped bodies at various angles of attack (see Fairlie 1980; Bippes & Turk 1983). The Reynolds numbers of these observed patterns are high (of order 10^5) but the flow patterns synthesized are at low Reynolds numbers

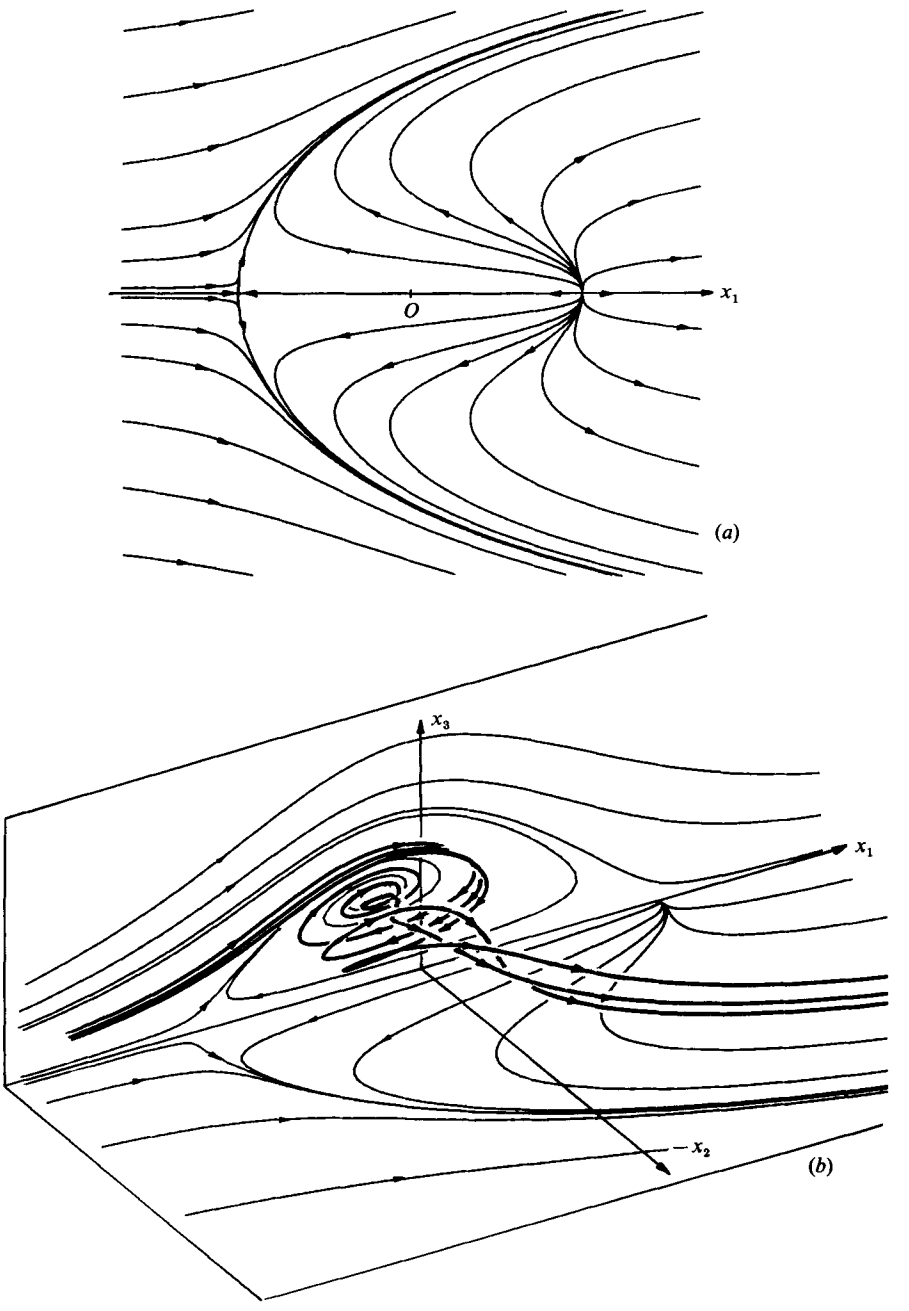

FIGURE 6. Symmetrical third-order U separation. (*a*) Surface flow pattern, i.e. limiting streamlines on the (x_1, x_2)-plane. (*b*) Oblique view with some out-of-plane trajectories added (shown as heavy lines).

(of order 10^2 or less). The Reynolds number here is based on the vorticity at the origin divided by viscosity, i.e. $Re = \eta(O)/\nu$. Nevertheless, in this preliminary investigation we have managed to synthesize patterns that are topologically similar to those observed (at least at the surface). It should be pointed out that the simple U separation synthesized here is third order. With the no-slip boundary conditions, this

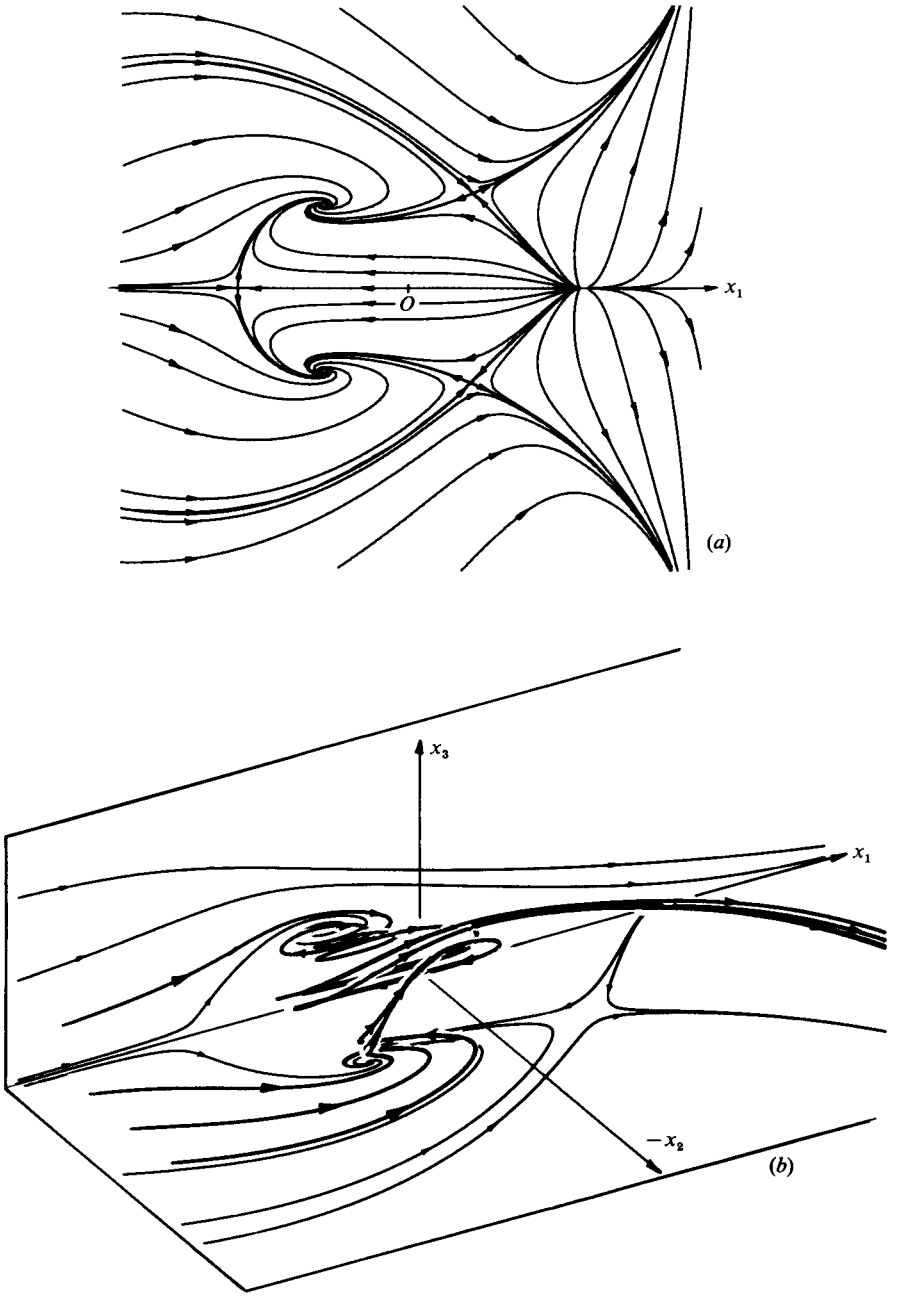

FIGURE 7. Symmetrical fourth-order owl-face of the second kind. (*a*) Surface flow pattern, i.e. limiting streamlines on the (x_1, x_2)-plane. (*b*) Oblique view with some out-of-plane trajectories added (shown as heavy lines).

represents creeping flow, i.e. no inertia force is present. One must go to at least fourth order to produce inertia forces. Again, as a check on the algorithm, the synthesized solution was used to generate boundary conditions on three mutually perpendicular planes passing through the origin. Using these boundary conditions (i.e. at $x_3 = 0$, $u_1 = u_2 = u_3 = 0$, and the values of u_i on the (x_2, x_3)- and (x_1, x_3)-planes) with the

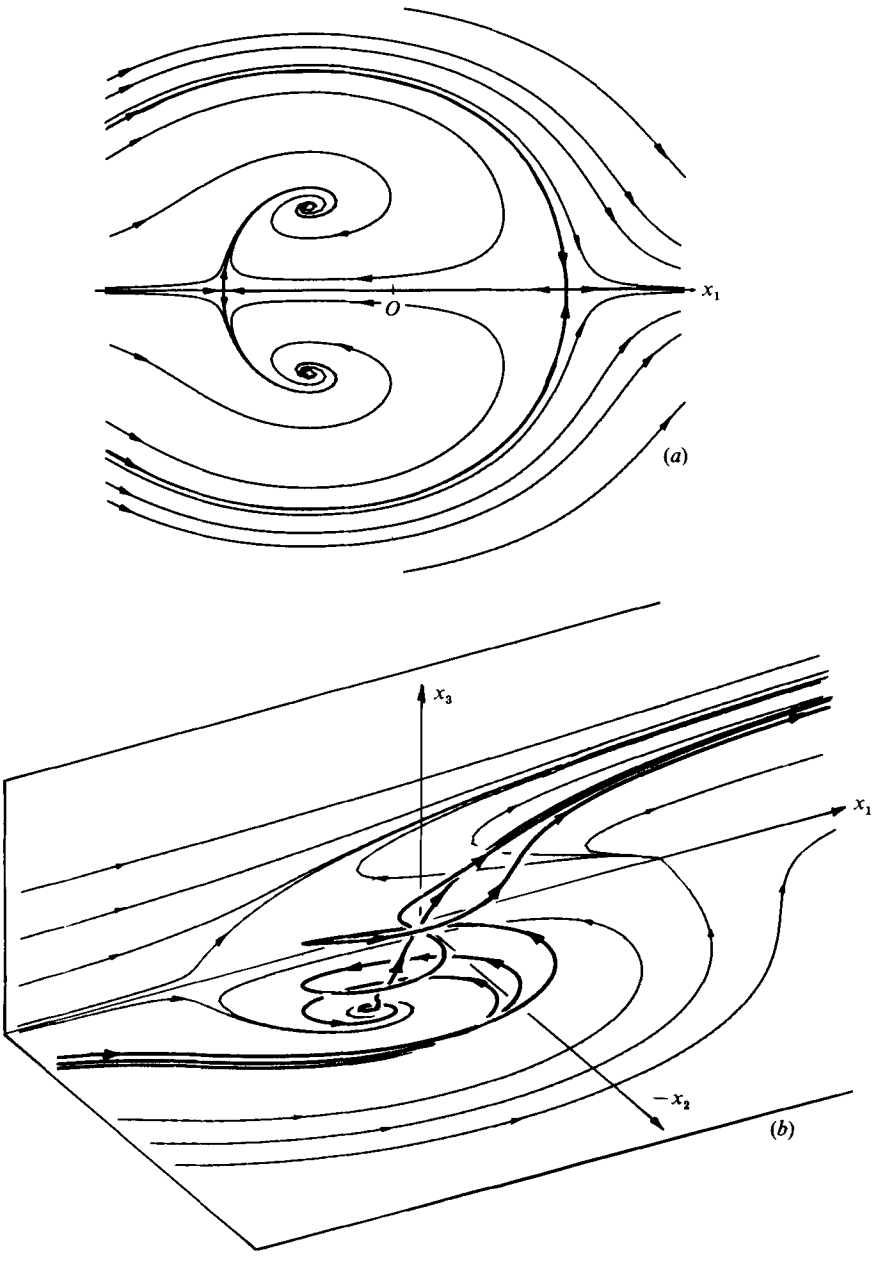

FIGURE 8. Symmetrical fifth-order owl-face of the first kind. (*a*) Surface flow pattern, i.e. limiting streamlines on the (x_1, x_2)-plane. (*b*) Oblique view with some out-of-plane trajectories added (shown as heavy lines).

algorithm, results were obtained which agreed with the synthesized solutions including the limiting surface streamlines (i.e. we successfully retrieved what we initially specified using an entirely different solution procedure).

In the synthesis of the separation bubbles given in figure 6, 7 and 8, the pattern was assumed to be symmetrical (u_1 and u_3 were assumed to be even in x_2 and u_2 was assumed to be odd in x_2). This assumption simplified the solution procedure.

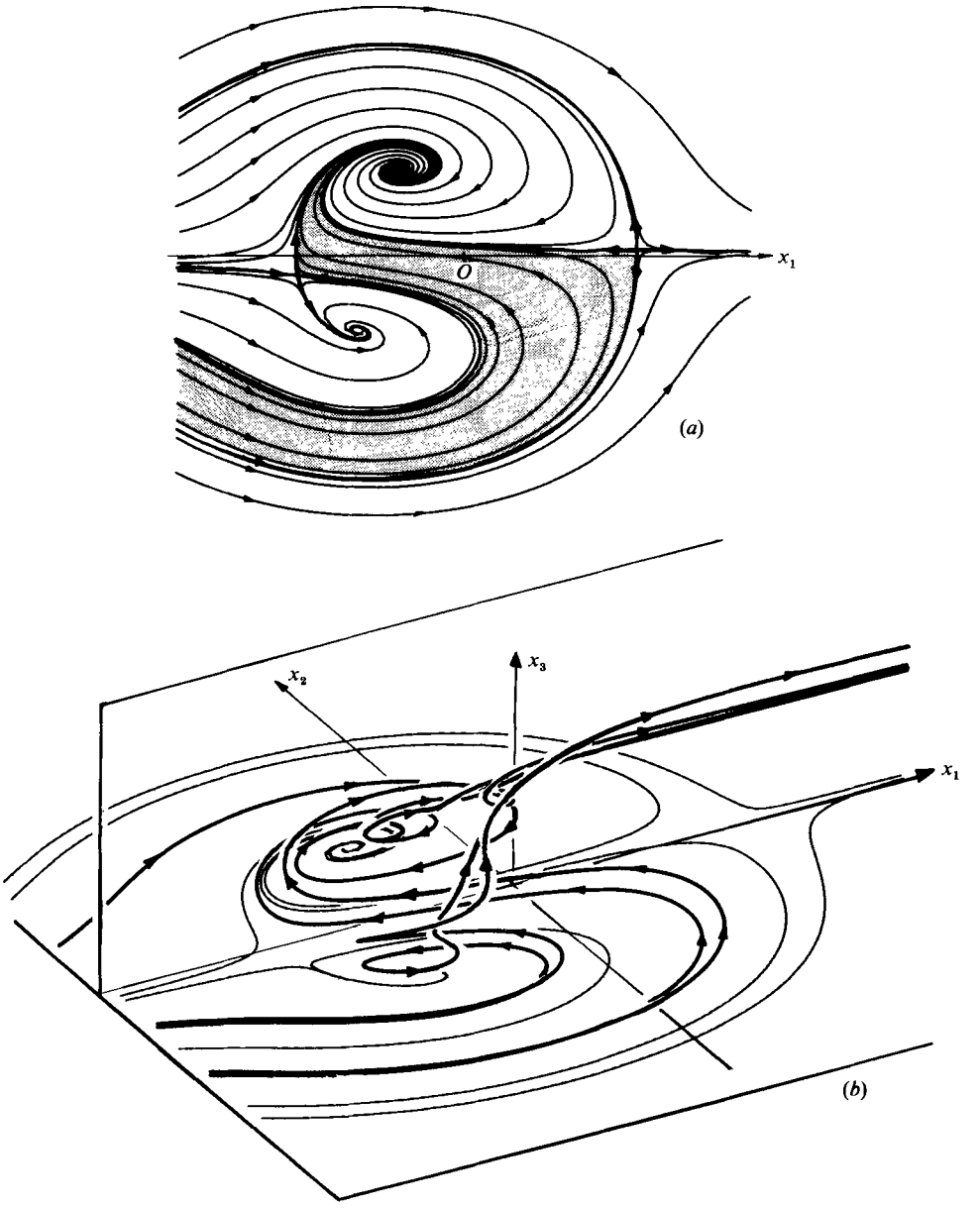

FIGURE 9. Unsymmetrical fifth-order owl-face of the first kind. (*a*) Surface flow pattern, i.e. limiting streamlines on the (x_1, x_2)-plane. (*b*) Oblique view with some out-of-plane trajectories added (shown as heavy lines).

Unsymmetrical solutions can be obtained by generating the canonical boundary conditions from the synthesized symmetrical solutions and perturbing the resulting boundary conditions on the (x_1, x_3)-plane so that the symmetry condition is violated. We then use the algorithm in combination with the new unsymmetrical canonical boundary conditions to solve for the three-dimensional flow pattern. This solution includes the limiting streamlines. This has been applied to the owl-face pattern of the first kind, and the resulting pattern is shown in figure 9. Note in figure 9 (*a*) how

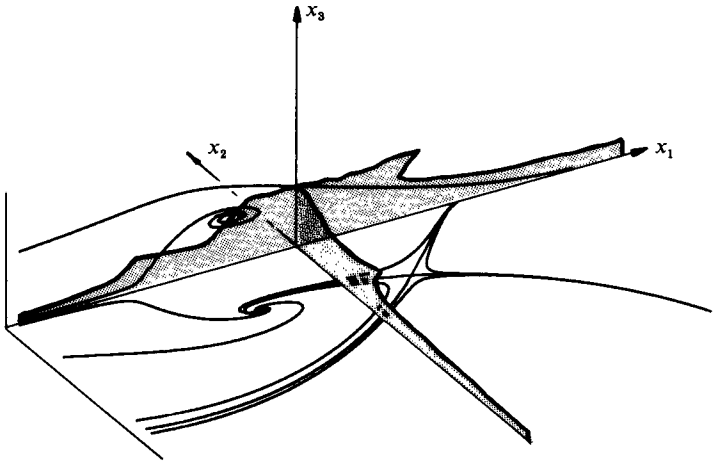

FIGURE 10. Region of accuracy on the (x_1, x_3)-plane and on the (x_2, x_3)-plane. The separation pattern is the symmetrical owl-face of the second kind as shown in figure 7.

fluid shown shaded on one side of the centreplane finds its way to the focus on the other side of the centreplane. This pattern has undergone a major change in topology since the original symmetrical pattern was structurally unstable, i.e. it has a saddle-to-saddle connection by a separatrix streamline (see Tobak & Peake 1982; Perry & Hornung 1984 regarding structural stability).

Regions of accuracy can also be computed for the various three-dimensional flow patterns using the method described in §3 using comparison 3. These are difficult to represent graphically. An example of the region of accuracy in the (x_1, x_3)- and (x_2, x_3)-planes is shown in figure 10 for the flow pattern shown in figure 7.

So far the authors have taken two-dimensional flow to ninth order and three-dimensional flow to fifth order. There is no difficulty in generating the equations to higher order. However, some labour is required in developing a solution strategy after the equations have been generated. We hope to pursue this to high orders. Perhaps ultimately this latter aspect of the work can be carried out using the computer, as was done with the former aspect.

6. Conclusions and discussions

An algorithm has been developed which enables the local Taylor-series-expansion solutions of the Navier–Stokes and continuity equations to be generated to arbitrary order. The various continuity and Navier–Stokes relationships between the various coefficients of the expansion can be generated quite easily by using a computer to do the necessary algebra.

The region of accuracy of the resulting local solutions can be found. For a given Reynolds number, the higher the order of the expansion the greater the region of accuracy. For a given order of expansion, the region of accuracy shrinks with Reynolds number. In principle the algorithm can be used for solving steady and unsteady problems by the specification of external boundary conditions. The algorithm has some very interesting properties if boundary conditions are specified on the coordinate planes passing through the origin of the expansion (the canonical boundary conditions). If the equations are solved in the correct sequence, all relationships effectively become linear and the solution can be determined without any iterative procedure.

The algorithm enables flow patterns to be synthesized. These synthesized patterns are known to be asymptotically exact solutions to the equations of motions close to the origin of the expansion and are valid in a finite zone with a certain accuracy. This synthesis is analogous to that carried out in classical hydrodynamics where a pattern with various required properties is constructed by an appropriate distribution of sources, sinks or point vortices. Here we are carrying out the construction of nonlinear viscous-flow patterns by the choice of an appropriate arrangement of critical points, and the solution strategy is such that we are solving analytically a set of linear equations by successive substitution. This alone, the authors believe, justifies the development of the algorithm. With these analytical solutions, the vorticity fields can be obtained and the topological properties of such fields have yet to be explored

Dallmann (1983) has initiated a study into the bifurcation processes which occur in flow patterns as various parameters are varied. Critical points move about, change their character and merge to form entirely different flow-pattern topologies. The algorithm developed here should form a useful basis for such studies.

This study was a joint project between the University of Melbourne and the Institut für experimentelle Strömungsmechanik, DFVLR, Göttingen. The authors wish to acknowledge fruitful discussions with Professor H. G. Hornung, who suggested that tensor analysis might be useful in this work. The financial assistance of the Australian Research Grant Scheme is also gratefully acknowledged.

REFERENCES

Bippes, H. & Turk, M. 1983 Oil flow patterns of separated flow on a hemisphere cylinder at incidence. *DFVLR Rep. No.* IB 222-83 A 07, Göttingen, West Germany.

Dallmann, U. 1983 Topological structures of three-dimensional flow separation. *DFVLR Rep. No.* IB 221-82 A 07, Göttingen, West Germany.

Fairlie, B. D. 1980 Flow separation on bodies of revolution at incidence. In *Proc. 7th Austr. Hydr. and Fluid Mech. Conf., Brisbane*, pp. 338–341.

Hornung, H. G. 1983 The vortex skeleton model for three-dimensional steady flows. Aerodynamics of vortical type flows in three dimensions. *AGARD Conf. Proc.* No. 342.

Hornung, H. G. & Perry, A. E. 1984 Some aspects of three-dimensional separation. Part I. Streamsurface bifurcations. *Z. Flugwiss. Weltraumforschung* **8**, 77–87.

Lighthill, M. J. 1963 Attachment and separation in three-dimensional flow. In *Laminar Boundary Layers* (ed. L. Rosenhead), pp. 72–82. Oxford University Press.

Oswatitsch, K. 1958 Die Ablösungsbedingung von Grenzschichten. In *Grenzschichtforschung* (ed. H. Goertler), pp. 357–367. Springer.

Perry, A. E. 1984*a* A study of degenerate and non-degenerate critical points in three-dimensional flow fields. *Forschungsbericht DFVLR-FB* 84-36, Göttingen, West Germany.

Perry, A. E. 1984*b* A series expansion study of the Navier–Stokes equations. *Forschungsbericht DFVLR-FB* 84–34, Göttingen, West Germany.

Perry, A. E. & Chong, M. S. 1986 A series expansion study of the Navier–Stokes equations with applications to three-dimensional separation patterns – A detailed treatment. *Rep.* FM-17. Mech. Engng Dept, University of Melbourne.

Perry, A. E., Chong, M. S. & Hornung, H. G. 1985 Local solutions of the Navier–Stokes equations for separated flows. *3rd Symp. on Numerical and Physical Aspects of Aerodynamic Flows, California State University, Long Beach, California.*

Perry, A. E. & Fairlie, B. D. 1974 Critical points in flow patterns. *Adv. Geophys.* B **18**, 299–315.

Perry, A. E. & Hornung, H. G. 1984 Some aspects of three-dimensional separation. Part II. Vortex skeletons. *Z. Flugwiss. Weltraumforschung* **8**, 155–160.

Tobak, M. & Peake, D. J. 1982 Topology of three-dimensional separated flows. *Ann. Rev. Fluid Mech.* **14**, 61–85.